Available online at www.sciencedirect.com

ScienceDirect

Procedia Engineering 96 (2014) 510 – 516

Procedia Engineering

www.elsevier.com/locate/procedia

Modelling of Mechanical and Mechatronic Systems MMaMS 2014

Model of Flexible Robot with Deformation Detection

Jiří Volech, Ladislav Mráz, Zbyněk Šika*, Michael Valášek[a]

[a]*CTU in Prague, Faculty of Mechanical Engineering, Technická 4, Praha 6, 166 07, Czech republic*

Abstract

The paper deals with the simulation of a concept performing the deformation measurement of a serial robot. The simulation model consist of two parts. The one of them is the model of the flexible robot with the flexibility concentrated in its gearboxes and its beams. The other one is the model of sensors measuring virtually the flexible deformations of the gearboxes and the arms. The rotary encoders are used for the gearboxes and the sensor consisting of the leaser emitter and the photodiodes measures the arms deformation. The deformation of the whole structure leads to an undesired error in the end-effector position control. Using this concept of measurement enables the compensation of this inaccuracy. The simulation model is used for the optimization of the additional measurement concept.

Peer-review under responsibility of organizing committee of the Modelling of Mechanical and Mechatronic Systems MMaMS 2014

Keywords: End-effector position; deformation measurement; dynamic model

1. Introduction

The machining with industrial robots is an attractive field of interest for the researchers. The robots are able to cover larger workspace, have a high movability and the process performing by them has a lower cost in comparison to the traditional machines. However, the robotic machining brings many issues which have to be addressed.

The one is the imperfect dimensions of the robot components which differ from the nominal ones. This phenomenon arises during the parts manufacturing and it is common for the robots as well as for the traditional machines. The similar situation is in the problem of thermal dilatations of the parts. These problems can be solved by calibration and by the ensuring of the work temperatures in the field of the negligible thermal deformations.

However one problem is more significant for the robots, since their stiffness is lower than the stiffness of the conventional machines. This issue needs a particular attention and the research in this field is rather intensive.

The way of prediction of the robot deformation is the development of a mathematical model of the flexibility or the direct experimental measurement of the deformations.

The project Advocut [1, 2] has showed several methods for the robots precision enhancement. The main source of the compliance represent the gearboxes of the robot, which have been equipped with the rotary sensors of deformation. However the flexibility of the arms play a non-negligible role and it has not been considered at all in this project.

Approaches described in [3, 7, 8, 9, 16] are based on the analytical prediction of the deformation of the robotic structure. The

* Zbyněk Šika. Tel.: +420-22435-7452
E-mail address: Zbynek.Sika@fs.cvut.cz

Peer-review under responsibility of organizing committee of the Modelling of Mechanical and Mechatronic Systems MMaMS 2014
doi:10.1016/j.proeng.2014.12.123

model of the flexibility is assembled, which parameters are experimentally determined. The problem of the deformations estimation based on the model is its inaccuracy, moreover, the experimental parameters determination requires a considerable effort devoted to a particular robot.

Another way is the on-line measurement of the tool centre point (TCP) position and its feedback compensation along the desired trajectory. Such an approach is presented in [4, 5]. The TCP position is determined using a serial measuring structure connected to a robot. The issue limiting this approach is the addition of the errors in the serial measuring structure and its connection to a robot represent a movability restriction. Moreover, only the Cartesian position of TCP is measured by the structure and there is no information about the orientation of the end-effector. This process has been used for the machine-tools only, not for the robots. However, similar approach has been adopted for the parallel-kinematic structure Tricept [6]. Again the Cartesian coordinates of the TCP have been measured, not the orientation. This concept shoved positive results in the serial production performing by Tricept. However the robot had to produce the first product on which the off-line measurement had been performed determining the errors. Afterwards, the compensation have been applied and the production continued with enhanced accuracy. Such an approach is appropriate for serial production, but not for a single machining task.

The connection of the precise stiffness model of the robot with the external position tracking is shoved in Comet project [10, 11, 12]. The external tracking system determined the trajectory deviation of the TCP and the compensation of the errors have been performed using a pizo-actuated mechanism with limited but fast movability. The work-piece have been attached to the piezo-system.

The project showed remarkable results. Some limitation can be in the restricted workspace dictated by the piezo-mechanism movability. Higher accuracy of the TCP measurement can be achieved by redundant tracking systems.

It is obvious from the abovementioned approaches, that the precise mathematical modelling of the structure in connection with the external measurement show the right way how to solve the problem of the robot compliance. A concept of the connection of the mathematical model with the external deformation measurement is presented in this paper. Its functionality is shown on the simulation results.

2. The dynamic model

The robot Mitsubishi RV-6S (Fig. 1.a) has been chosen as a pattern for the mathematical model. The robot consist of seven parts (including the fixed base) and has six degrees of freedom. The gearboxes are considered to be flexible as well as the longer arms.

The dynamic model of the robot (Fig. 1.b) has been created using the composite method for the flexible mechanisms [13]. The recursive method is based on the system description by two sets of coordinates. One set of them are the traditional relative coordinates representing the movement in the joints of the robot. The deformation of the arms is described by the modal coordinates. The deformation of the flexible arms is evaluated using their modal shapes of deformation. The modal coordinates are then the coefficients of the linear combinations of these shapes.

Moreover, the flexibility of the gearboxes is considered. The relative coordinates are introduce for the position description of the rotors, which are connected to the arms by gearboxes stiffness.

The resulting structure description is following. The relative coordinates representing the joint rotation are $\boldsymbol{q} = [q_1, q_2, q_3, q_4, q_5, q_6]^T$, the modal coordinates describing the deformations are: $\boldsymbol{E} = [\boldsymbol{e_3}, \boldsymbol{e_5}]$. The vectors $\boldsymbol{e_3}$ and $\boldsymbol{e_5}$ representing the deformation of the arms 3 and 5. The other arms are considered as rigid because of their dimensions. Finally the coordinates $\boldsymbol{q_M} = [q_{1M}, q_{2M}, q_{3M}, q_{4M}, q_{5M}, q_{6M}]^T$ represent the position of the motors rotors.

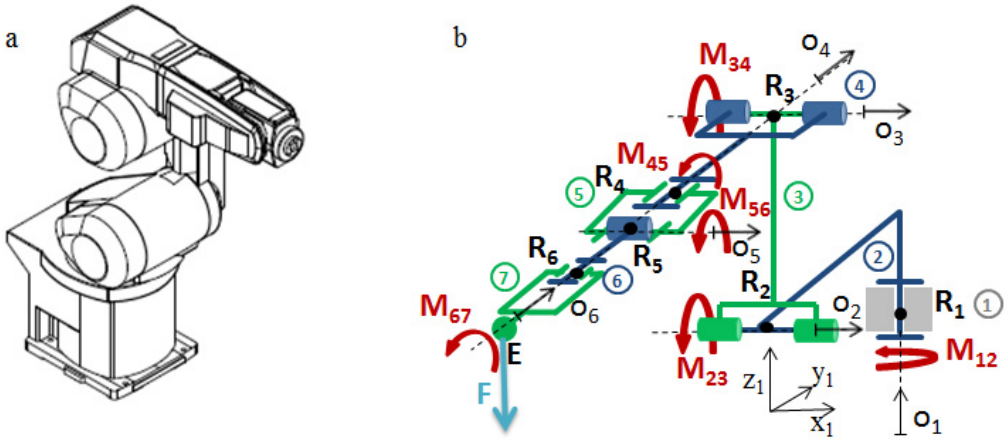

Fig. 1. (a) Robot Mitsubishi RV-6S; (b) Robot model.

Using the recursive formalism for the flexible bodies [13] the final system of equations of motion (EOM) is obtained:

$$\begin{bmatrix} \boldsymbol{M^R(q,E)} & \boldsymbol{M^{RF}(q,E)} & \boldsymbol{0} \\ \boldsymbol{(M^{RF}(q,E))^T} & \boldsymbol{M^F(q,E)} & \boldsymbol{0} \\ \boldsymbol{0} & \boldsymbol{0} & \boldsymbol{M^M} \end{bmatrix} \begin{bmatrix} \ddot{\boldsymbol{q}} \\ \ddot{\boldsymbol{E}} \\ \ddot{\boldsymbol{q}}_{\boldsymbol{M}} \end{bmatrix} = \begin{bmatrix} \boldsymbol{Q^R(q,\dot{q},E,\dot{E},q_M,\dot{q}_M)} \\ \boldsymbol{Q^F(q,\dot{q},E,\dot{E},q_M,\dot{q}_M)} \\ \boldsymbol{Q^M(q,\dot{q},E,\dot{E},q_M,\dot{q}_M)} \end{bmatrix} \tag{1}$$

The symbol $\boldsymbol{M^R}$ represents the part of mass matrix related to the „rigid“ motion, $\boldsymbol{M^F}$ is the part of the mass matrix representing the „flexible“ motion and $\boldsymbol{M^{RF}}$ represents the interconnection of them. The symbol $\boldsymbol{M^M}$ represents the mass matrix of the rotors. The symbols on the right-hand side are the corresponding generalized force vectors.
With the notation $\boldsymbol{y} = [\boldsymbol{q}, \boldsymbol{E}, \boldsymbol{q_M}]^T$, the system (1) can be easily described by:

$$\boldsymbol{M_y}\ddot{\boldsymbol{y}} = \boldsymbol{Q_y} \tag{2}$$

And denoting $\boldsymbol{x_1} = \boldsymbol{y}$ and $\boldsymbol{x_2} = \dot{\boldsymbol{y}}$ the system of differential equations of the first order can be obtained:

$$\dot{\boldsymbol{X}} = \begin{bmatrix} \dot{\boldsymbol{x_1}} \\ \dot{\boldsymbol{x_2}} \end{bmatrix} = \begin{bmatrix} \boldsymbol{x_2} \\ \boldsymbol{M_y^{-1}Q_y} \end{bmatrix} \tag{3}$$

The model of robot dynamics based on the EOM (3) have been assembled in the Matlab-Simulink environment. The parameters of the model had to be estimated according the material of the robot parts and their dimensions. The eigen-modes of the flexible arms have been obtained using the FEM analysis. The resulting robot model have been further equipped by a cascade control enabling the positioning. The scheme is depicted in Fig. 2.

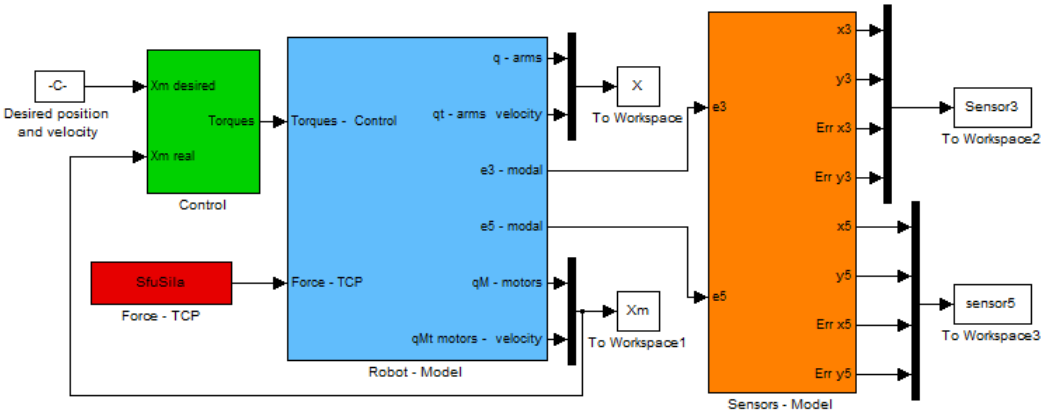

Fig. 2. The simulation model.

The model is used for the simulation of the deformations behaviour during some working process of the robot. The measuring of the deformation is performed by the virtual laser-photodiode system described in the following section.

3. Laser detection of the deformations

The four-quadrant-sensor 4QD (see Fig. 3) is described in this paper. The sensor consists of photodiodes (quadrants) A, B, C, D. These quadrants are equal and separated from each other with small gaps. Its operation principle is conversion of the light energy to the electrical energy. Photodiodes transform incoming laser beam to the currents I_a, I_b, I_c a I_d, afterwards they are transform to the relatively voltage levels V_a, V_b, V_c a V_d, by the operational amplifier. Voltage level generated on each quadrant is proportional equal to the optical energy illuminating its surface [17, 18].

To illustration the position sensing operation of the sensor, it is assumed that the spot, which is illuminated by laser beam, has perfectly circular shape with uniform distribution of power on the 4QD sensor. Generally the laser spot can appear anywhere on the sensing area as shown in Fig. 3. The initial position is if x=y=0, then laser falls into the perfect centre of the detector, which is the cross point of the two gap lines, then the output currents I_a, I_b, I_c a I_d from all the photodiodes are the same. The spot displacement along the x-axis or y-axis of the detector will be detected as a relative change between these four current outputs and then removed in the fine tracking control loop.

These currents are calculated in following manner in order to calculate the so called pointing error, relative to the centre of the detector:

$$E_x = K_x \frac{(I_a+I_d)-(I_b+I_c)}{I_a+I_b+I_c+I_d} = K_x \frac{(V_a+V_d)-(V_b+V_c)}{V_a+V_b+V_c+V_d} \quad (4)$$

$$E_y = K_y \frac{(I_a+I_b)-(I_c+I_d)}{I_a+I_b+I_c+I_d} = K_y \frac{(V_a+V_b)-(V_c+V_d)}{V_a+V_b+V_c+V_d} \quad (5)$$

Where K_x and K_y are the correlation coefficient of the x- and y-axis directions respectively.

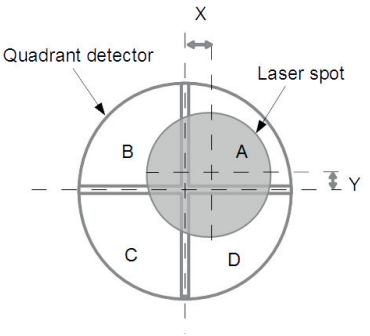

Fig. 3. Relative position of the laser spot.

3.1. Sensor transfer characteristics.

When using the position sensor, there are several constraints, which must be considered. The Laser spot has to be larger than the gap between active areas and smaller than the detector's active area. Second, the total position range is limited to the size of the active area of the sensor. Another problem which have to be considered is that detection range increases with spot size, while position resolution decreases. This is because a given movement in a large spot size create a much smaller differential signal than the same movement in the smaller beam. The solution of how large the laser beam must be to give a reasonable positional resolution with still acceptable measurement range will be done in the future.

3.2. Modeling of the 4QD sensor.

The outputs characteristics of the each sensor quadrants are directly related to the energy of the laser beam that falls on them. For the purpose of making the mathematical model of the 4-quadrant detector sensor, two main parts are considered: The first part represents the energy of the illuminated area of the each photodiode by incoming laser beam. And the second is the shape of the incoming laser beam. In reality the energy of the laser beam is not uniformly distributed over whole illuminated area. For our purpose we assuming that the laser beam has uniform intensity distribution, and ideal circular shape spot. The energy of each illuminated area is given by the following equations:

$$S_A = \frac{\pi * r^2}{4} + xy + \frac{x}{2}\sqrt{r^2-x^2} + \frac{y}{2}\sqrt{r^2-y^2} + \frac{r^2}{2}\left[\sin^{-1}\left(\frac{x}{r}\right) + \sin^{-1}\left(\frac{y}{r}\right)\right] \quad (6)$$

$$S_B = \frac{\pi * r^2}{4} - xy - \frac{x}{2}\sqrt{r^2-x^2} + \frac{y}{2}\sqrt{r^2-y^2} - \frac{r^2}{2}\left[\sin^{-1}\left(\frac{x}{r}\right) + \sin^{-1}\left(\frac{y}{r}\right)\right] \quad (7)$$

$$S_C = \frac{\pi * r^2}{4} + xy - \frac{x}{2}\sqrt{r^2-x^2} - \frac{y}{2}\sqrt{r^2-y^2} - \frac{r^2}{2}\left[\sin^{-1}\left(\frac{x}{r}\right) + \sin^{-1}\left(\frac{y}{r}\right)\right] \quad (8)$$

$$S_D = \frac{\pi * r^2}{4} - xy + \frac{x}{2}\sqrt{r^2-x^2} - \frac{y}{2}\sqrt{r^2-y^2} + \frac{r^2}{2}\left[\sin^{-1}\left(\frac{x}{r}\right) + \sin^{-1}\left(\frac{y}{r}\right)\right] \quad (9)$$

Where S_a, S_b, S_c, S_d, are the illuminated area of the four quadrants respectively, x and y are the displacements of the spot centre and the 4QD centre and r is the radius of the laser beam [19]. The pointing errors E_x and E_y are also calculated using the each illuminated area of the four quadrants by following formulas:

$$E_x = K_x \frac{(I_a+I_d)-(I_b+I_c)}{I_a+I_b+I_c+I_d} = K_x \frac{(S_a+S_d)-(S_b+S_c)}{S_a+S_b+S_c+S_d} \quad (10)$$

$$E_y = K_y \frac{(I_a+I_b)-(I_c+I_d)}{I_a+I_b+I_c+I_d} = K_y \frac{(S_a+S_b)-(S_c+S_d)}{S_a+S_b+S_c+S_d} \quad (11)$$

If we substitute (6)-(9) to the (10) and (11), we obtain mathematical model of the 4QD sensor which computes the pointing errors and the displacement, as follows:

$$E_x = K_x \frac{(S_a+S_d)-(S_b+S_c)}{S_a+S_b+S_c+S_d} = K_x \frac{1}{\pi r^2}\left[2x\sqrt{r^2-x^2} + 2r^2 \sin^{-1}\left(\frac{x}{r}\right)\right] \quad (12)$$

$$E_y = K_y \frac{(S_a+S_b)-(S_c+S_d)}{S_a+S_b+S_c+S_d} = K_y \frac{1}{\pi r^2}\left[2y\sqrt{r^2-y^2} + 2r^2 \sin^{-1}\left(\frac{y}{r}\right)\right] \quad (13)$$

3.3. Measurement

The parallel structure of the laser beam and sensor frame with the robot arms (Fig. 4) has been chosen as the appropriate model for the simulation

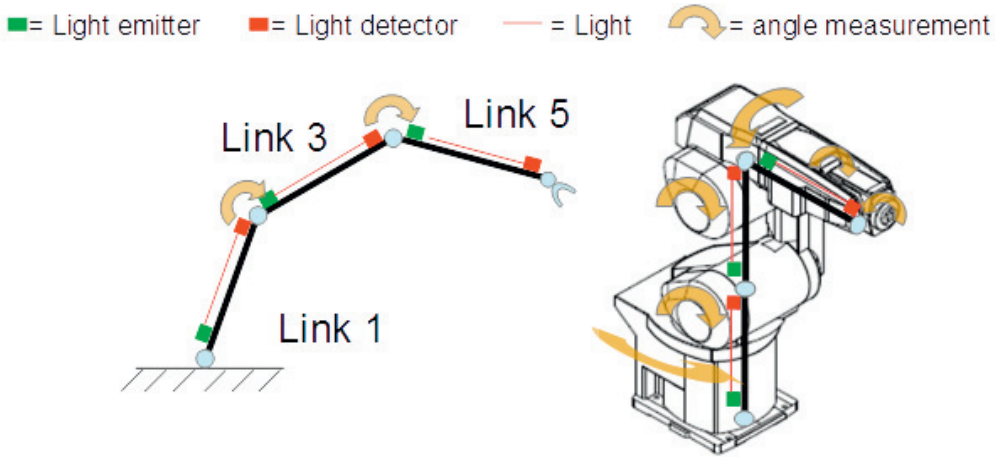

Fig. 4. The parallel laser concept.

The measuring method provide the feedback control signal through on-line measurement of the structural deflection of all links. This eliminates the necessities of dynamics calculation in the quasi-static manner. For the feedback control system it is essential to predict the end-effector tracking and positioning errors caused by the link and transition deflection [14, 15].

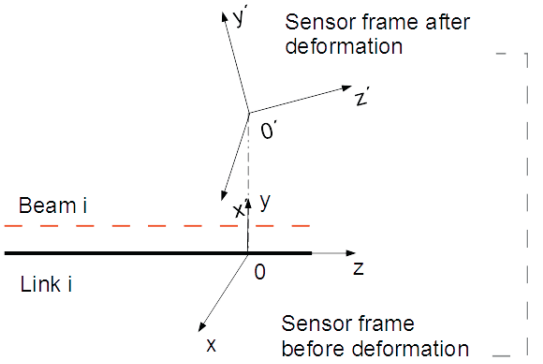

Fig. 5. The change of the sensor position caused by the deformation.

Before the model of real structure with 3 dimensional sensor will be created, the simulations with 2 dimensional sensor has been carried out, measured only x=Δu and y=Δv deflection of each link (Fig. 5), Δw is relatively smaller and can be neglected. Suppose that the link i (i=1, 2, 3,…., n) has small translational displacements (Δu, Δv, 0) at the tip, it is derived from the theory of error perturbation [3], that the end-effector has the positioning errors as follows:

$$\begin{pmatrix} dx^n \\ dy^n \\ dz^n \end{pmatrix} = \sum_{i=1}^{n} B_i^T \begin{pmatrix} \Delta u_i \\ \Delta v_i \\ 0 \end{pmatrix} = \sum_{i=1}^{n} \begin{pmatrix} I_{ix} & I_{iy} & I_{iz} \\ m_{ix} & m_{iy} & m_{iz} \\ n_{ix} & n_{iy} & n_{iz} \end{pmatrix} \begin{pmatrix} \Delta u_i \\ \Delta v_i \\ 0 \end{pmatrix} \quad (14)$$

Where (dx^n, dy^n, dz^n) represent the robot translational positioning errors in the end effector frame, respectively, and the parameters being concerned are related to the nominal kinematics.

4. The simulations results

The models of the robot dynamics and the model of the deformation sensing described above have been connected together in the Simulink environment in order to simulate the real experiment of the deformation measurement. The two dimensional PSD S1880 from Hamamatsu company has been chosen as a sensing PSD. It has the photosensitive area of 12x12 mm and laser beam with 3 mm radius. The end point of the robot's model has been loaded with force of 100 N pointing vertically down, in the negative direction of the global axis z_1 (Fig. 1.b). Then the resulting deformations and stabilization in the new equilibrium position of the endpoint of the arm 3 and 5 was captured by the sensors and are depicted in Fig. 6.

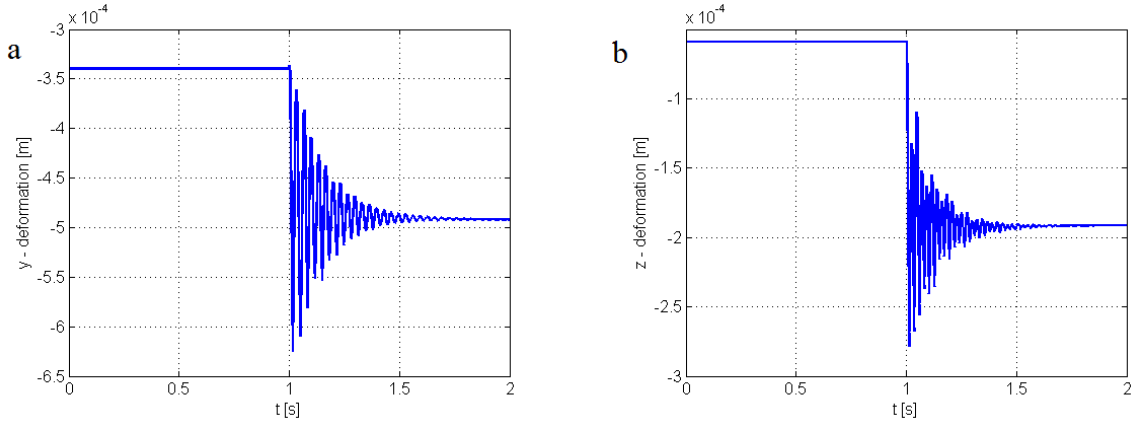

Fig. 6. (a) Endpoint deformation of arm 3; (b) Endpoint deformation of arm 5

The force is applied in the time 1 s and causes the main deformation of the links in the direction of global axis y_1 (link 3) and z_1 (link 5). It is obvious, that the force excite the vibrations which amplitude is decreasing and finally they are damped out and the new equilibrium position is achieved.

5. Conclusion

The deformations of a robotic structure play a reasonable role if the structure is loaded and the precise position control is desired. The paper describes a concept of the additional measurement of the deformations and the possibility of their compensation. The flexible gearboxes are usually considered to be the main source of the deformation of the structure leading to undesired inaccuracy in position control. However, the flexibility of the links cannot be neglected.

The dynamic model of the robot has been assembled and introduced in this paper. It has been modelled the flexibility of the gearboxes and the links. The model has been equipped with the virtual additional sensors for determination of the elements deformations. The simulation results show the behaviour of the deformation in time. The information about them can be further used in order to compensate the errors in the TCP position control.

Acknowledgements

The authors appreciate the kind support by the grant **GA13-39057S** "**Position Feedback Based Stiffness Increase of Robots by Redundant Measurement**" of the Czech Science Foundation.

References

[1] www.advocut.de
[2] Abele, E. (ed.): ADVOCUT, Abschlussbericht BMBF – Verbundprojekt, Adaptive vollserielle Werkzeugmaschine mit hochintegriertem mechatronischen Fräsmodul zur HSCBearbeitung, PTW, TU Darmstadt, Darmstadt 2007, ISBN: 987-3-87525-256-9.
[3] E. Abele, M. Weigold, S. Rothenbücher: Modeling and Identification of an Industrial Robot for Machining Applications, Annals of the CIRP Vol. 56/1/2007, pp. 387-390
[4] A. Verl, N. Croon, C. Kramer, T. Garber and G. Pritschow: Force Free Add-on Position Measurement Device for the TCP of Parallel Kinematic Manipulators, CIRP Annals - Manufacturing Technology Volume 55, Issue 1, 2006, pp. 407-410
[5] Zhuang, H.: Self-calibration of parallel mechanisms with a case study on Stewart platforms, IEEE Trans. On Robotics and Automation, 13(1997), 3, pp. 387-397.
[6] Neumann, K.E.: Tricept Applications, In: Neugebauer, R. (ed.): Development Methods and Application Experience of Parallel Kinematics The 3rd Chemnitz Parallel Kinematics Seminar PKS 2002, IWU FhG, Chemnitz 2002, pp. 547-551.

[7] P. Zengxi, H. Zhang: Improving Robotic Machining Accuracy by Real-time Compensation, ICROS-SICE International Joint Conference, Fukuoka, 2009, pp. 4289-4294.
[8] N. R. Slavkovic, et al: Cartesian Compliance Identification and Analysis of an Articulated Machining Robot, FME Transactions, 2013, vol. 41, pp. 83-95.
[9] O. Sörnmo, B. Olofsson, A. Robertsson, R. Johansson: Increasing Time-Efficiency and Accuracy of Robotic Machining Processes Using Model-Based Adaptive Force Control, 10th IFAC Symposium on Robot Control – SYROCO 2012, Dubrovnik, 2012, pp. 543-548.
[10] C. Lehmann, M. Pellicciari, M. Drust, J. W. Gunnink: Machining with industrial robots: the COMET project approach, Communications in Computer and Information Science Volume 371, 2013, pp 27-36.
[11] A. Puzik, C. Meyer, A. Verl: Robot Machining with additional 3-D-Piezo-Actuation-Mechanism for Error Compensation, Robotics (ISR), 2010 41st International Symposium on and 2010 6th German Conference on Robotics (ROBOTIK), 7-9 June 2010, pp. 1-7.
[12] O. Sörnmo, et al: Increasing the Milling Accuracy for Industrial Robots Using a Piezo-Actuated High Dynamic Micro Manipulator, The 2012 IEEE/ASME International Conference onAdvanced Intelligent Mechatronics, Kaohsiung, 2012, pp. 104-110.
[13] T. Vampola, M. Valášek: Composite Rigid Body Formalism for Flexible Multibody Systems. Multibody System Dynamics, 2007, Volume 18, Issue 3, pp 413-433
[14] P. Zengxi, H. Zhang: Improving Robotic Machining Accuracy by Real-time Compensation, ICROS-SICE International Joint Conference, Fukuoka, 2009, pp. 4289-4294.
[15] S.K. Tso, X.S. Wang, J.Z. Zhang: Sensor-based deflection modeling and compensation control of a flexible robotic manipulator, IEEE International Conference on Systems, Man, and Cybernetics, 1997, Computational Cybernetics and Simulation, 1997, vol.4, pp. 3780-3785.
[16] B. L. Wilkerson, D. Giggenbach, B. Epple: Concepts for fast acquisition in optical communications systems, SPIE Vol.6304, 2006.
[17] H. Zhen, S. Zhengxun, T. Shoufeng, X. Zhao, S. Hongfei, J. Huilin: Modeling of Fine Tracking Sensor for Free Space Laser Communication Systems, Photonics and Optoelectronics, 2009. SOPO 2009. Symposium on, vol., no., pp.1,4, 14-16 Aug. 2009 doi: 10.1109/SOPO.2009.5230084.
[18] M. Cotsaftis: Advances in Factories of the Future, Cim and Robotics (Manufacturing Research and Technology), 1993, ISBN-10: 0444898565.
[19] Pacific Silicon Sensor Quadrant Series Datasheet, http://www.pacificsensor.com.